



HAL
open science

Mn/Ca ratios of *Ammonia tepida* as a proxy for seasonal coastal hypoxia

Jassin Petersen, Christine Barras, Antoine Bézos, Carole La, Caroline Slomp, Filip J.R. Meysman, Aurélia Mouret, Frans Jorissen

► **To cite this version:**

Jassin Petersen, Christine Barras, Antoine Bézos, Carole La, Caroline Slomp, et al.. Mn/Ca ratios of *Ammonia tepida* as a proxy for seasonal coastal hypoxia. *Chemical Geology*, 2019, 518, pp.55-66. 10.1016/j.chemgeo.2019.04.002 . hal-02398525

HAL Id: hal-02398525

<https://hal.science/hal-02398525>

Submitted on 22 Oct 2021

HAL is a multi-disciplinary open access archive for the deposit and dissemination of scientific research documents, whether they are published or not. The documents may come from teaching and research institutions in France or abroad, or from public or private research centers.

L'archive ouverte pluridisciplinaire **HAL**, est destinée au dépôt et à la diffusion de documents scientifiques de niveau recherche, publiés ou non, émanant des établissements d'enseignement et de recherche français ou étrangers, des laboratoires publics ou privés.



Distributed under a Creative Commons Attribution - NonCommercial 4.0 International License

1 Mn/Ca ratios of *Ammonia tepida* as a proxy for seasonal coastal 2 hypoxia

3
4

5 Jassin Petersen^{1*}, Christine Barras¹, Antoine Bézos¹, Carole La¹, Caroline P. Slomp²,
6 Filip J.R. Meysman^{3,4}, Aurélie Mouret¹, and Frans J. Jorissen¹

7 ¹LPG UMR CNRS 6112, University of Nantes, University of Angers, UFR Sciences, 2 Boulevard
8 Lavoisier, 49045 Angers Cedex 01, France

9 ²Department of Earth Sciences (Geochemistry), Faculty of Geosciences, Utrecht University,
10 Princetonlaan 8a, 3584 CB Utrecht, The Netherlands

11 ³Department of Biology, University of Antwerp, Universiteitsplein 1, BE- 2610 Wilrijk, Belgium

12 ⁴Department of Biotechnology, Delft University of Technology, 2629 HZ Delft, The Netherlands

13 *now at: Institute of Geology and Mineralogy, University of Cologne, Zùlpicher Str. 49a, 50674
14 Cologne, Germany

15

16 **Abstract**

17

18 Climate variability has major implications for marine geochemical cycles and biogenic
19 carbonate production. Therefore, past climate-driven changes in marine environments are
20 often inferred from geochemical data of the marine carbonate archive. Proxy calibration
21 studies are essential for the reconstruction of such past environmental changes. Here, we
22 use the geochemical composition of living specimens of the benthic foraminifer *Ammonia*
23 *tepada* at three sites in a seasonally hypoxic (oxygen concentration < 63 $\mu\text{mol/L}$) marine
24 coastal system (Lake Grevelingen, the Netherlands) to explore the use of Mn/Ca as a proxy
25 for coastal hypoxia. The study is based on samples from three stations along a depth
26 transect, that have contrasting seasonal cycles of Mn²⁺ concentrations in the pore water of
27 the surface sediment. Specifically, the sediment and pore water geochemistry of the three
28 stations in Lake Grevelingen show increased Mn²⁺ concentrations in late winter/spring,
29 combined with increased Mn refluxing in summer, which are due to cable bacteria activity
30 and bottom water hypoxia/anoxia, respectively.

31 Laser Ablation-ICP-MS (LA-ICP-MS) allowed a comparison of Mn/Ca ratios of different parts
32 of the benthic foraminiferal test. Our results show that higher Mn/Ca ratios are registered at
33 the deepest station, which experiences the longest and most severe seasonal periods of
34 hypoxia/anoxia. Additionally, the signal preserved in the central part of the benthic
35 foraminiferal tests, which is thought to reflect the entire calcification history of the analysed
36 specimen, appears to be driven by high pore water Mn²⁺ concentrations due to cable bacteria

37 activity in late winter/spring. Conversely, high Mn/Ca ratios in the last chambers reflect
38 increased Mn refluxing in the surface sediment due to summer hypoxia/anoxia. Thus, Mn/Ca
39 ratios of *A. tepida* give insight into the complex spatial and temporal variability of pore water
40 manganese.

41

42 Keywords: coastal hypoxia; benthic foraminifera; geochemical proxy development; redox-
43 sensitive elements; biomineralization; micro-analytical techniques

44

45 **1. Introduction**

46 In coastal areas, the development of seasonally hypoxic zones (water bodies with O₂
47 concentration < 63 μmol/L or 2 mg/L) has become a wide-spread phenomenon in response
48 to increasing riverine nutrient input and rising temperatures (e.g., Rabalais et al., 2002;
49 Gilbert et al., 2010; reviews in Diaz and Rosenberg, 2008; Rabalais et al., 2010, 2014;
50 Breitburg et al., 2018; Fennel and Testa, 2018). In Europe, hypoxic periods have been
51 observed in the Baltic Sea and in the northern Adriatic Sea (e.g., Jorissen et al., 1992;
52 Conley, 2002; Conley et al., 2007; Meier et al., 2011). Hypoxia negatively impact marine
53 benthic fauna and alter sediment biogeochemical cycles, strongly affecting the entire
54 ecosystem functioning (e.g., Middelburg and Levin, 2009). Direct measurements of oxygen
55 concentrations are relatively scarce, and are generally restricted in time and space, but some
56 tools make it possible to follow the oxygenation history of coastal ecosystems in the recent
57 sediment record (e.g., Cooper and Brush, 1991; Barmawidjaja et al., 1995; Itoh et al., 2003;
58 Zillén et al., 2008). Such historical studies can inform us in more detail about the onset of
59 seasonal hypoxia in pre-anthropogenic times, and its sensitivity to climate change. Yet, it still
60 remains a challenge for the scientific community to develop reliable proxies for seasonal
61 hypoxia allowing the reconstruction of the historical record.

62 Several geochemical proxies have been proposed, based on redox-dependent elements,
63 such as manganese, uranium, vanadium and molybdenum (Breit and Wanty, 1991; Adelson
64 et al., 2001; Tribovillard et al., 2004; McManus et al., 2005; Algeo and Lyons, 2006; Scholz et
65 al., 2017; van Helmond et al., 2018; review in Tribovillard et al., 2006). In environments
66 where concentrations of bottom water oxygen (BWO) and the input of Mn bearing suspended
67 matter are sufficient, soluble manganese (Mn²⁺) is released through reductive dissolution of
68 Mn (oxyhydr)oxides when they are buried in (or mixed into) deeper, anoxic sediment. The
69 Mn²⁺ can then diffuse upwards and precipitate as Mn (oxyhydr)oxides in the oxygenated
70 surface sediment, leading to recycling of Mn in the sediment. Mn²⁺ can also diffuse
71 downwards and precipitate as Mn carbonate (e.g., Middelburg et al., 1987; Slomp et al.,
72 1997). Because under hypoxic conditions, Mn cycling will take place closer to the sediment

73 surface compared to oxygenated conditions, manganese incorporated in benthic
74 foraminiferal calcite could be a suitable proxy for marine benthic hypoxia (Reichert et al.,
75 2003; Munsel et al., 2010; Glock et al., 2012; Groeneveld and Filipsson, 2013; Koho et al.,
76 2015, 2017; McKay et al., 2015; Petersen et al., 2018; Barras et al., 2018; Guo et al., 2019).
77 The latter studies show that benthic foraminifera register environmental Mn^{2+} concentrations
78 in their tests. A complicating factor is that in case of anoxia, Mn^{2+} oxidation takes place
79 entirely in the bottom water (e.g., Sulu-Gambari et al., 2017), and the Mn^{2+} concentration in
80 the surface sediments is no longer sufficient for detectable incorporation into the benthic
81 foraminiferal test. Barras et al. (2018) have demonstrated that under hypoxic conditions,
82 seawater Mn^{2+} linearly scales with the Mn/Ca ratio of tests of cultured *Ammonia tepida*, a
83 coastal benthic foraminifer. Petersen et al. (2018) have additionally shown that the variability
84 of successive single chamber Mn/Ca ratios of the same species is not only related to intrinsic
85 variability (due to biological processes during calcification), but also reflects temporal and
86 spatial (environmental) variability of pore water Mn^{2+} . Furthermore, Petersen et al. (2018)
87 evoked active or passive migration of the foraminifera in the surface sediment to explain part
88 of the observed Mn/Ca variability within single specimens. The latter observations were
89 made in Lake Grevelingen, a coastal ecosystem in the Netherlands with seasonally hypoxic
90 to anoxic BWO concentration, which is also the sampling area of the present study (Fig. 1).

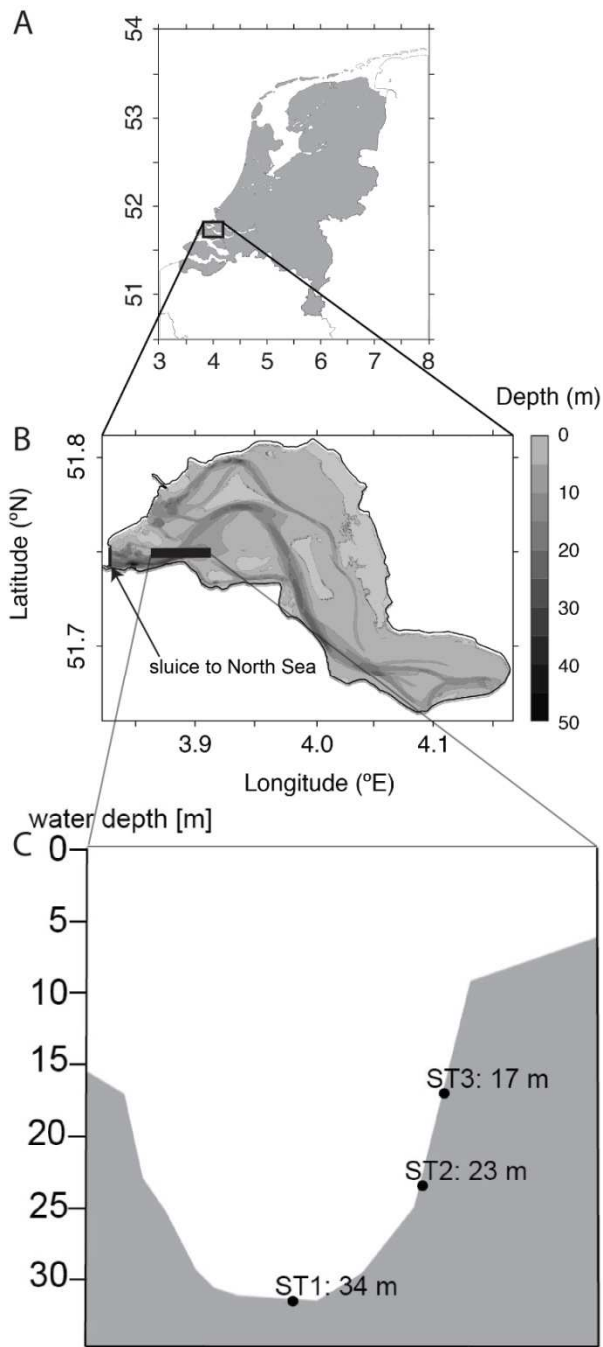
91 Lake Grevelingen is a former branch of the Rhine-Meuse-Scheldt delta. This artificial saline
92 lake was formed after the construction of dams in 1964 (connection to the river inlets were
93 cut off) and 1971 (connection to the North Sea was cut off), and has only a minor seawater
94 inflow through two small sluices (Bannink et al., 1984). The salty bottom waters (salinity 31-
95 32.5, Hagens et al., 2015) of the lake are subject to seasonal hypoxia and anoxia, which
96 strongly affects the benthic ecosystem (Seitaj et al., 2015; Sulu-Gambari et al., 2016a). In
97 2012, the water column was sampled monthly at three stations in the Den Osse basin in the
98 main channel of Lake Grevelingen (water depth: 34 m, 23 m and 17 m for stations ST1, ST2
99 and ST3, respectively, Fig. 1). The deepest station is most affected by seasonal
100 hypoxia/anoxia; it shows a longer duration of hypoxia and is characterized by lower BWO
101 concentrations in summer and early autumn than the shallower stations. It has been shown
102 that the seasonal pattern of sediment geochemical cycling is substantially influenced by the
103 presence of cable bacteria, which increase in activity from the shallowest to the deepest
104 station (Seitaj et al., 2015). These bacteria, which perform long-distance electron transport,
105 are mainly active in winter and early spring (Seitaj et al., 2015, 2017). Due to the specific
106 metabolic activity of cable bacteria, a strong enrichment of Mn^{2+} and Mn (oxyhydr)oxides
107 occurs in the surface sediment in late winter and spring (Sulu-Gambari et al., 2016b). The
108 electrogenic sulfur oxidation by the cable bacteria induces a chain of biogeochemical

109 reactions involving dissolution of iron mono-sulfides (FeS), reduction of Mn (oxyhydr)oxides
110 by upward diffusing Fe²⁺, leading to accumulation of Mn²⁺ in the pore water. Mn oxides are
111 built up in the oxic layer directly below the sediment water-interface (SWI) by the upward
112 diffusing Mn²⁺ (Seitaj et al., 2015; Sulu-Gambari et al., 2016a,b). Additional Mn oxides are
113 supplied through deposition of Mn-bearing suspended matter (Sulu-Gambari et al., 2017).

114 Live benthic foraminifera (recognised by CellTracker Green, CTG, Bernhard et al., 2006)
115 were sampled at three stations, and show assemblages strongly dominated by *Ammonia*
116 *tepida* and *Elphidium excavatum*. The living specimens of *Ammonia tepida* in Lake
117 Grevelingen are strongly dominated by phylotype T6, which is one of the three phylotypes
118 occurring along the European Atlantic coast (Richirt et al., 2019). Nevertheless, since it
119 remains very difficult to separate these phylotypes morphologically, we use the name
120 *Ammonia tepida*, knowing that it designates a species complex rather than a single biological
121 species.

122 Here, we present Mn/Ca ratios measured by laser ablation ICP-MS (LA-ICP-MS) on
123 specimens of *Ammonia tepida* sampled at the three different stations and relate these to the
124 geochemistry of the environment. The benefit of Lake Grevelingen is that a large dataset on
125 water column geochemistry combined with pore water and sediment geochemistry is
126 available for the same sites where the specimens of *A. tepida* were sampled (Hagens et al.,
127 2015; Seitaj et al., 2015, 2017; Sulu-Gambari et al., 2016a,b, 2017a). Therefore, it is possible
128 to compare the measured Mn/Ca ratios in the foraminiferal tests with corresponding
129 concentrations of Mn²⁺ in the pore water. The analyses focused on the penultimate and
130 antepenultimate chambers (n-1 and n-2), supposed to record pore water Mn²⁺ concentration
131 prior to sampling, and the central part of the test (n-c), supposed to give an averaged signal
132 of the life span of the specimen. We will investigate whether the incorporated manganese in
133 the foraminiferal test has a potential to reconstruct spatial and temporal variability in pore
134 water Mn²⁺. The ultimate aim of this study is to develop a proxy for the extent and intensity of
135 seasonal hypoxia in coastal ecosystems.

136



137

138 Figure 1. Location map of Lake Grevelingen and the three sampling stations in this study. A: map of the Netherlands. B:
 139 bathymetry of Lake Grevelingen, the sluice giving access to the North Sea is situated at the most western end of the lake. C:
 140 depth cross-section of the Den Osse basin (W-E) with locations of stations ST1, ST2 and ST3. Modified from Hagens et al.
 141 (2015).

142

143

144

145

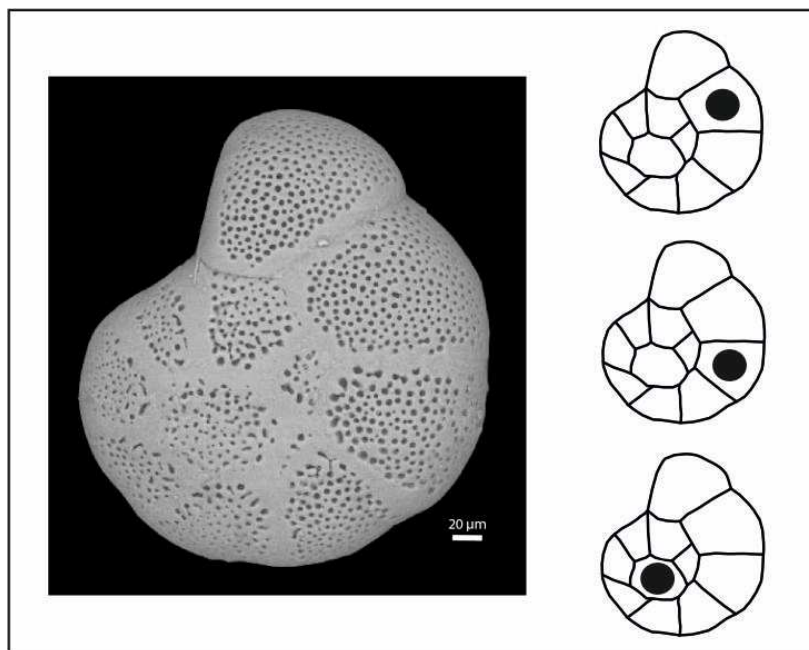
146 2. Material and methods

147 2.1. Mn/Ca ratios of *Ammonia tepida* from Lake Grevelingen

148 The three sampling stations are located along a depth transect in the Den Osse basin, the
149 former estuarine channel towards the North Sea (Fig. 1A,B). Water depth decreases
150 gradually from station ST1, in the deepest part of the basin (34 m), to 23 m at ST2 and 17 m
151 at ST3 (Fig. 1C). At ST1, ST2 and ST3, short sediment cores (~40 cm) with ~20 cm of
152 overlying bottom water were collected with a gravity corer (UWITEC, Austria) and Plexiglas®
153 core-liners (6 cm inner diameter; 60 cm length, Sulu-Gambari et al., 2017). For pore water
154 measurements, one core was sliced at high resolution (0.5 cm slices over 10 cm) in a N₂-
155 purged glovebag (Sulu-Gambari et al., 2016a). Cores for the study of live benthic
156 foraminifera were taken bimonthly, on the same dates that cores for sediment geochemistry
157 were sampled, starting in January 2012. Foraminiferal communities were studied in two
158 depth intervals (0-0.5 cm and 0.5-1 cm, Richirt et al., in prep.). Live foraminifera were
159 discriminated from dead specimens using the CTG staining method (Bernhard et al. 2006). In
160 all the samples where living foraminifera were found, the morphospecies *Ammonia tepida*
161 and *Elphidium excavatum* were strongly dominant. Here we measured the elemental
162 composition of calcite tests of *A. tepida* (size fraction 150-315 µm, 0-0.5 cm interval) sampled
163 in July 2012 at ST1, ST2 and ST3. The test size was measured on SEM images as the
164 maximum diameter using the image processing software ImageJ (Schneider et al., 2012).
165 The cleaning of all specimens, in order to remove sediment adherences (Barker et al., 2003),
166 included rinsing three times with ultra-pure water, followed by one rinse in methanol and
167 three final rinses in ultra-pure water. During each rinse, samples were slightly agitated with a
168 vortex machine (Petersen et al., 2018). Guo et al. (2019) showed that this type of physical
169 cleaning in combination with LA-ICP-MS yields Mn/Ca ratios of live benthic foraminifera
170 comparable to solution analysis (by ICP-MS) of specimens which have undergone a protocol
171 involving oxidative and reductive cleaning. In fact, the integration of contamination from the
172 surface of the test into the calcite Mn/Ca signal is avoided by the data treatment of LA-ICP-
173 MS analysis involving the screening of indicator elements such as Al (e.g., Koho et al., 2015;
174 Barras et., 2018; Petersen et al., 2018; Guo et al., 2019).

175 We measured the elemental composition of single chambers of the calcite tests using LA-
176 ICP-MS, i.e., an ArF excimer laser (193 nm, Analyte G2, Teledyne Photon Machines)
177 coupled to a quadrupole ICP-MS (Varian Bruker 820-MS). Ablations were performed in a
178 HelEx II 2-Volume Cell with He as carrier gas, a laser energy density of 0.91 J/cm² and a 4
179 Hz repetition rate. Spot sizes were adapted to the chamber size in order to maximize the
180 amount of ablated material, and they varied typically between 40 and 85 µm in diameter.
181 Variable spot sizes have been used in other studies of foraminiferal tests and are not thought

182 to influence elemental fractionation (Eggins et al., 1998; Diz et al., 2012; de Nooijer et al.,
183 2014; Petersen et al., 2018). Analyses were performed preferably in the penultimate (n-1)
184 and antepenultimate (n-2) chambers as well as in the central part of the test (n-c, see Fig. 2
185 for location of ablation spots on the test). In some specimens with broken last chambers, it
186 could not be established precisely which chamber was measured (n-u). The data were
187 calibrated against NIST SRM 612 which was ablated in raster mode with the same repetition
188 rate and energy density as the foraminiferal samples and a 65 μm spot size. The calibration
189 using NIST SRM 612 was shown by Petersen et al. (2018) to yield accurate results and
190 fractionation effects were monitored using different reference materials. External
191 reproducibility for Mn/Ca was determined using carbonate reference materials USGS MACS-
192 3 and NFHS (NIOZ, Netherlands Institute of Sea Research, foraminifera in-house standard,
193 Mezger et al., 2016) and was 1.3 % and 4.5 %, respectively (calculated as $2 \times \text{RSE}$, relative
194 standard error). Details of the LA-ICP-MS measurements, as well as of data treatment and
195 quality control are reported in Petersen et al. (2018). Similar to the latter study, integrated
196 intervals displaying < 10 data points (24 ablations) or a Mn signal $<$ Limit Of Quantification
197 (LOQ, 6 ablations) were discarded from the data presented here. The final dataset includes
198 71 individual Mn/Ca measurements.



199
200 Fig 2. Left: SEM image of *A. tepida* specimen (presumably phylotype T6 based on morphological distinction as
201 shown by Richirt et al., 2019) from Lake Grevelingen (image taken at SCIAM, University of Angers). Right:
202 Sketches to show location of LA-ICP-MS spot analysis on penultimate chamber (top), antepenultimate chamber
203 (middle) and central part of test (bottom).

204

205 **2.2. Statistical analyses**

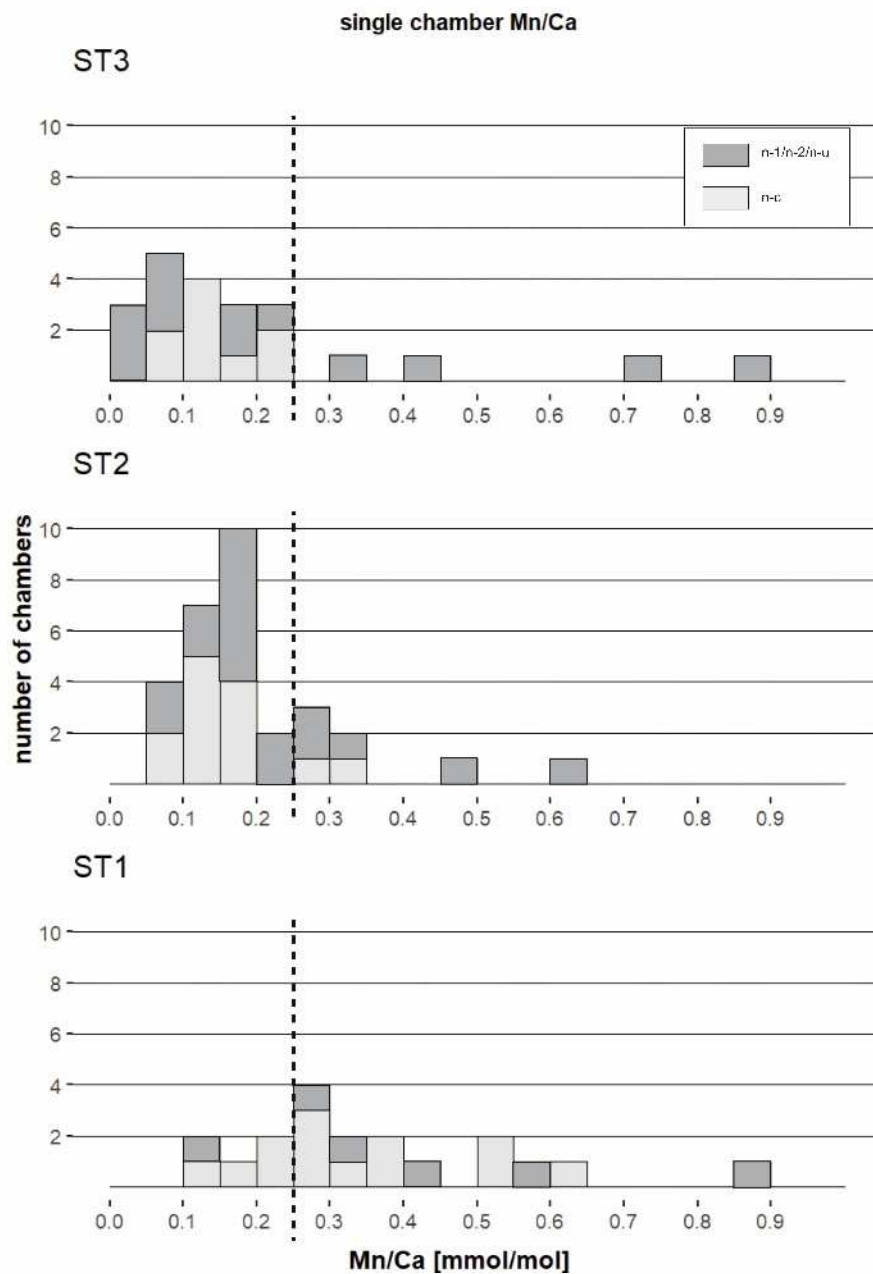
206 We performed statistical analyses under R (R Core Team, 2016) and we used the package
207 ggplot2 for graphical representation (Wickham, 2009). We used the Shapiro-Wilk test to
208 verify if data are normally distributed. For normally distributed data, we performed ANOVA
209 and t-tests with the Bonferroni adjustment as post-hoc test to compare datasets. For data
210 likely not to follow a normal distribution we performed a Kruskal-Wallis test and Wilcoxon-
211 Mann-Whitney as post-hoc test. In all cases, a *p* value below 0.05 was considered as
212 significant.

213

214 **3. Results: Mn/Ca ratios of *Ammonia tepida***

215 In order to compare the Mn/Ca ratios of specimens from the three stations, we chose
216 samples from July 2012, for two reasons. Firstly, because at ST1, a rich population of
217 *Ammonia tepida* was only found in May and July 2012, and secondly, because inter-station
218 differences in BWO concentration were maximal in this month. Thirteen specimens were
219 analysed for ST3 and ST1, respectively, and fourteen specimens for ST2. The maximum
220 diameter of each specimen shows that specimens of ST1 were significantly smaller than
221 specimens from ST2 and ST3 (Tab. 1, *p* values in Tab. 2).

222 All Mn/Ca ratios of individual chambers and tests are presented in Figure S2. Histograms for
223 each station for all measurements of single chambers and of the central part of the test (Fig.
224 3) indicate an increased number of high Mn/Ca ratios at ST1 compared to ST2 and ST3. In
225 fact, for this dataset which is not likely to follow a normal distribution *p* values for Kruskal-
226 Wallis and Wilcoxon-Mann-Whitney as post-hoc test confirm that there is a significant
227 difference for ST1 compared to ST2 and ST3 (not the case for ST2 and ST3, Tab. 2). Also
228 the mean Mn/Ca per specimen is significantly higher in ST1 compared to the other two
229 stations (0.36 ± 0.12 mmol/mol, mean \pm SD, for ST1 versus 0.18 ± 0.08 mmol/mol and 0.20
230 ± 0.15 mmol/mol for ST2 and ST3, respectively, Fig. 4A, *p* values in Tab. 3). There is no
231 significant difference between the three stations considering the Mn/Ca ratio of the
232 penultimate chamber, or of the combined n-1 and n-2 chambers (Fig. 4B/C, ANOVA *p* value
233 = 0.404 and 0.138, respectively). The measurements made in the central part of the test (Fig.
234 4D) yield significantly higher Mn/Ca ratios for ST1 compared to the other two stations (*p*
235 values in Tab. 3).

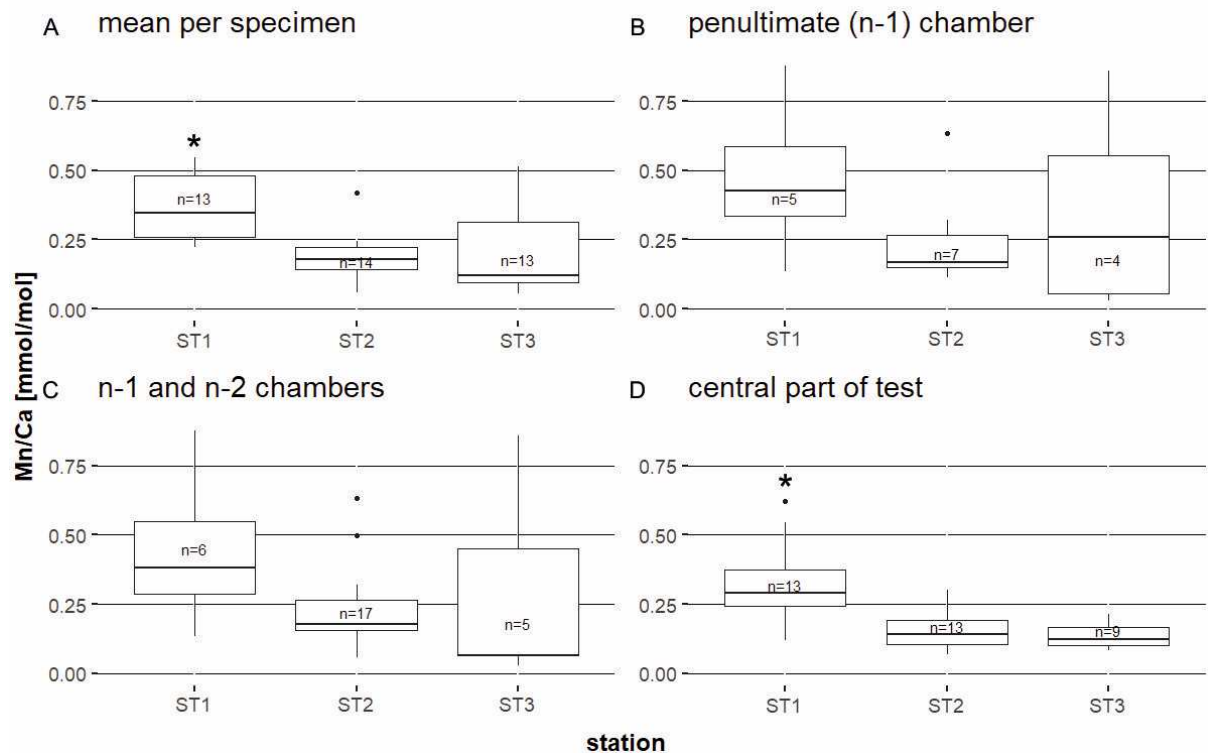


236

237 Figure 3. Histograms for all Mn/Ca measurements (individual chambers in dark grey, and central part of the test in light grey) for
 238 the three stations (bin width= 0.05 mmol/mol). Kruskal-Wallis test p value < 0.001 (for data of n-1/n-2/n-u and n-c combined).

239 Wilcoxon-Mann-Whitney post-hoc test p values: < 0.001 (ST1 vs ST2), < 0.001 (ST1 vs ST3) and 0.220 (ST2 vs ST3). Dashed
 240 line indicating 0.25 mmol/mol (see section 3 for explanation).

241



242

243 Figure 4. Boxplots of Mn/Ca ratios for all specimens of *A. tepida* from stations ST1 (34 m), ST2 (23 m) and ST3 (17 m) sampled
 244 in July 2012. A: mean per specimen (n indicates number of specimens). B: penultimate chamber (n indicates number of single
 245 chamber ablations, also in C and D). C: n-1 and n-2. D: central part of test. Data for n-u (n = 8) not represented. Significant
 246 differences for ST1 compared to ST2 and ST3 are indicated by *.

247 Table 1. Results (mean \pm SD) regarding test size (maximum diameter) and Mn/Ca ratios for all stations. Comparison of mean per
 248 test (including n-u), penultimate chamber (n-1), n-1 and n-2 chambers together and central part of test. In case of significant
 249 difference for value of ST1 compared to values of ST2 and ST3, value of ST1 is written in bold (p values in Tab. 2 and Tab. 3).

	Test size [μ m]	Mn/Ca mean per test [mmol/mol]	n	Mn/Ca n-1 [mmol/mol]	n	Mn/Ca n-1/n-2 [mmol/mol]	n	Mn/Ca central part [mmol/mol]	n
ST1	319 \pm58	0.36 \pm0.12	13	0.47 \pm 0.28	5	0.44 \pm 0.26	6	0.33 \pm0.15	13
ST2	376 \pm 63	0.18 \pm 0.08	14	0.25 \pm 0.18	7	0.22 \pm 0.15	17	0.16 \pm 0.07	13
ST3	407 \pm 36	0.20 \pm 0.15	13	0.35 \pm 0.39	4	0.29 \pm 0.36	5	0.14 \pm 0.05	9

250

251 Table 2. Lower left: Results for post-hoc t-test (p value, calculated with Bonferroni correction) for comparison of test size
 252 between the three stations (p value for ANOVA is 0.002). Upper right: Results for post-hoc test (p value, Wilcoxon-Mann-
 253 Whitney post-hoc test) for comparison of single chamber Mn/Ca ratios between the three stations as shown in Fig. 3 (p value for
 254 Kruskal-Wallis test is $<$ 0.001). Significant results in bold, a p value below 0.05 was considered significant.

	ST1	ST2	ST3
ST1		$<$ 0.001	$<$ 0.001
ST2	0.027		0.220
ST3	$<$ 0.001	0.444	

255

256

257 Table 3. Results for post-hoc test (p value, Wilcoxon-Mann-Whitney post-hoc test) for comparison of Mn/Ca ratios between the
 258 three stations for mean per specimen (lower left, in black; p value for Kruskal-Wallis test is < 0.001) and central part of test
 259 (upper right, in blue; p value for Kruskal-Wallis test is < 0.001). Significant results in bold, a p value below 0.05 was considered
 260 significant.

	ST1	ST2	ST3
ST1		< 0.001	< 0.001
ST2	< 0.001		0.512
ST3	0.006	0.402	

261

262

263 The histograms for each station (Fig. 3) show that the majority of values of single chamber
 264 Mn/Ca ratios were between 0-0.25 mmol/mol for stations ST2 and ST3. At ST1 there were
 265 no measurements smaller than 0.1 mmol/mol and a majority between 0.1-0.4 mmol/mol (Fig.
 266 3). High Mn/Ca ratios in benthic foraminifera are thought to reflect increased Mn^{2+}
 267 concentrations in the foraminiferal microhabitat, resulting from reductive dissolution of Mn
 268 (oxyhydr)oxides either due to hypoxic BWO conditions or intensive cable bacteria activity. As
 269 the preferred microhabitat of *A. tepida* is situated at or just below the surface of the sediment
 270 (Thibault de Chanvalon et al., 2015; Cesbron et al., 2016), it is expected that most of the
 271 calcified chambers are not subject to high pore water Mn^{2+} concentrations under oxic
 272 conditions. Consequently, only chambers calcified slightly deeper in the sediment or in the
 273 presence of increased Mn^{2+} concentrations in the surface sediment due to hypoxic conditions
 274 or cable bacteria activity would display such a high Mn/Ca. The geochemical data for the
 275 three stations (Sulu-Gambari et al., 2016a,b, 2017) show that a pore water Mn^{2+}
 276 concentration of $\sim 30 \mu\text{mol/L}$ is only reached in the bottom water in July 2012 at ST1, during
 277 strong hypoxia (Fig. S1). When using the D_{calcite} determined by Barras et al., 2018, for *A.*
 278 *tepada*, see supp. mat., this value should correspond to a foraminiferal Mn/Ca ratio of 0.25
 279 mmol/mol. Consequently, we used this value as a threshold to distinguish between high
 280 (calcite formed during hypoxia or production of Mn^{2+} by cable bacteria) and low Mn/Ca
 281 (foraminiferal calcite precipitated under oxic conditions and absence of cable bacteria).

282 We present for each station the number of specimens with low or high Mn/Ca (following this
 283 Mn/Ca threshold of 0.25 mmol/mol) in the latest analysed chambers (n-1, n-2 and n-u),
 284 and/or in the central part of test (n-c) in Table 4 (and Figure 5). At station ST3, nine out of
 285 thirteen specimens had low Mn/Ca (≤ 0.25 mmol/mol) in all chambers whereas four out of ten
 286 specimens had high values (> 0.25 mmol/mol) in at least one of the latest calcified chambers
 287 (counting only specimens for which reliable results for one of the later chambers were
 288 obtained). No specimens with high values in the central part of test were observed. At ST2,
 289 nine out of fourteen specimens showed low Mn/Ca in all chambers. Three of eleven

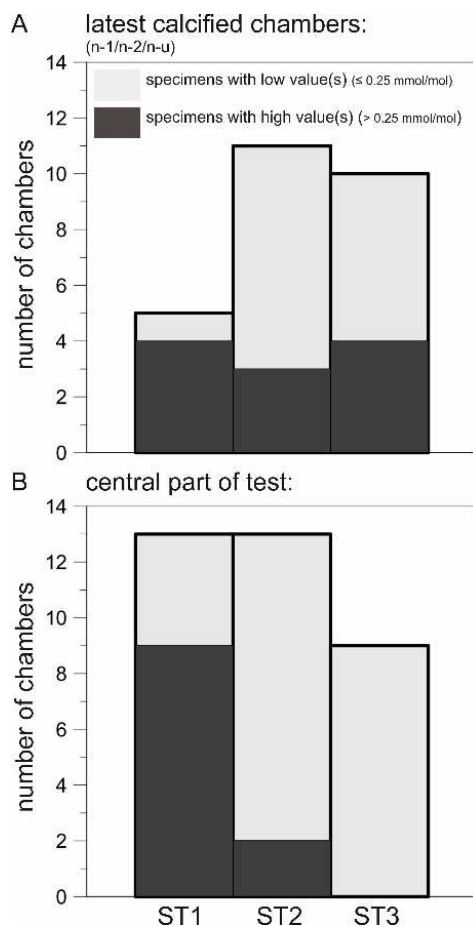
290 specimens had high Mn/Ca in one of the latest chambers and not in n-c, whereas two out of
 291 thirteen specimens showed elevated Mn/Ca ratios in n-c and not in the latest chambers. No
 292 specimens had high Mn/Ca both in the latest chambers and in the central part of test. At
 293 ST1, only two out of thirteen specimens yielded exclusively low Mn/Ca ratios. Four out of five
 294 specimens showed high Mn/Ca in at least one of the latest chambers and nine out of thirteen
 295 specimens had high Mn/Ca in the central part of test.

296

297 Table 4. Specimens with high Mn/Ca (> 0.25 mmol/mol) in comparison to total number of specimens, counting only specimens
 298 for which reliable results for the concerned chambers or part of the test were obtained.

	No high values	High values in n-1/n-2/n-u	High values in n-c
ST1	2/13	4/5	9/13
ST2	9/14	3/11	2/13
ST3	9/13	4/10	0/9
total	20/40	11/26	11/35

299



300

301 Figure 5. Specimens with high Mn/Ca ratios in comparison to total number of specimens measured for each station (data in Tab.
 302 4). A: Latest calcified chambers (n-1, n-2, n-u). B: Central part of test.

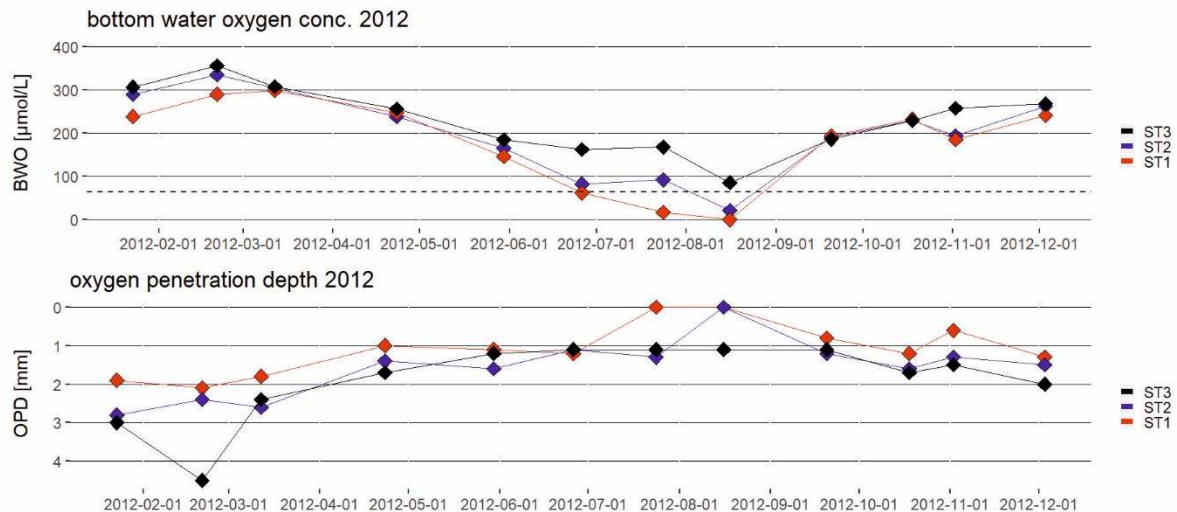
303

304 **4. Discussion**

305 **4.1. Environmental conditions in the study area**

306 **4.1.1. Oxygen variations in the bottom and pore waters**

307 In order to present our approach to disentangle the different processes behind Mn/Ca
308 variability of *Ammonia tepida* from Lake Grevelingen, we need first to explain the variations
309 of the environmental parameters in this study area. Results for the 2012 monthly campaigns
310 show that the water column was stratified from late spring (May) and during summer in
311 response to atmospheric temperature changes and a density gradient caused by the rapid
312 warming of surface waters (Hagens et al., 2015; Seitaj et al., 2017). The water column
313 remained stratified until September when stormy conditions induced a mixing of surface and
314 deeper waters (Hagens et al., 2015). The oxygen concentrations of the bottom waters
315 changed in phase with this stratification pattern; in winter BWO concentrations were
316 maximal, whereas bottom waters became oxygen depleted in summer (Fig. 6A). Sediment
317 oxygen uptake and the degradation of autochthonous and allochthonous organic matter
318 (OM) contributed to the decrease of oxygen concentration in the water column (Hagens et
319 al., 2015; Seitaj et al., 2017), leading to a decrease in the oxygen penetration depth (OPD;
320 the depth in the sediment below which O₂ concentration is < 1 μmol/L, Fig. 6B; Seitaj et al.,
321 2017). At the deepest station ST1 there was a hypoxic season of 2 to 2.5 months with
322 approximately two weeks of anoxia (Fig. 6A) during which the OPD decreased to zero,
323 meaning that there was an oxygen-free sediment in late summer at this station. At the
324 intermediate station ST2 hypoxia lasted for 1 to 1.5 months, and oxygen was absent in the
325 sediment only in August. The hypoxic period started later at ST2 than at ST1. Finally, at the
326 shallowest station ST3, oxygen levels remained above the hypoxia threshold throughout the
327 summer of 2012. The OPD was, at all three stations, slightly deeper in winter than in summer
328 (Fig. 6B). In conclusion, BWO concentration in the basin showed seasonal hypoxia to anoxia
329 which varied in intensity and duration as a function of water depth (Seitaj et al., 2017).



330

331 Figure 6. A: BWO concentration for stations ST1 (34 m), ST2 (23 m) and ST3 (17 m) with indicated sampling dates in 2012. The
 332 dashed line indicates the threshold for hypoxic conditions (63 $\mu\text{mol/L}$). B: Oxygen Penetration Depth for ST1, ST2 and ST3
 333 measured from sediment cores sampled on the same dates in 2012 as water column parameters. Data from Hagens et al.
 334 (2015) and Seitaj et al. (2017).

335

336 4.1.2 Sediment geochemistry

337 During the same monthly sampling campaigns in 2012 the pore water and solid-phase
 338 sediment geochemistry was also analysed. This large data set has been presented
 339 previously by Seitaj et al. (2015, 2017) and Sulu-Gambari et al. (2016a,b, 2017a). Despite
 340 the strong seasonal oxygen depletion in Lake Grevelingen, the occurrence of free sulfide in
 341 the bottom water (euxinia) is likely prevented or at least delayed, due to the presence of
 342 cable bacteria (Seitaj et al., 2015). The metabolic activity of these filamentous bacteria
 343 involves an electrical coupling between oxygen reduction at the sediment surface and sulfide
 344 oxidation in the deeper suboxic sediment via long-distance electron transport (Malkin et al.,
 345 2014; Meysman et al., 2015; Nielsen et al., 2010; Pfeffer et al., 2012). The sulfide oxidation
 346 induces both carbonate and FeS dissolution, which releases Fe^{2+} into the pore water as
 347 initially only demonstrated in laboratory experiments (Rao et al., 2016; Risgaard-Petersen et
 348 al., 2012). Similar processes occur in Lake Grevelingen; Sulu-Gambari et al. (2016a,b)
 349 demonstrated that the Fe^{2+} is released and diffuses upwards, and that a major proportion is
 350 oxidised by manganese oxides (input of Mn from the water column, Sulu-Gambari et al.,
 351 2016b). Mn oxides are supplied to the sediment surface through deposition of suspended
 352 matter from the water column. This supply is an important prerequisite for the impact of cable
 353 bacteria activity on the Mn cycle in winter (Sulu-Gambari et al., 2016b). In fact, Sulu-Gambari
 354 et al. (2016b, 2017) show a strong enrichment of solid-phase (total) Mn in the sediment
 355 surface in winter/early spring compared to summer months at all three stations. In

356 winter/early spring the reductive dissolution of Mn oxides by Fe^2 leads to the mobilisation of
357 Mn^{2+} (Reed et al., 2011; Thamdrup et al., 1994), and to distinct Mn^{2+} pore water peaks below
358 the OPD (Fig. S1, Sulu-Gambari et al., 2016a,b). Rao et al. (2016) additionally proposed that
359 substantial amounts of Mn^{2+} are released during CaCO_3 dissolution (induced by the cable
360 bacteria). In our study area, cable bacteria activity was assessed with microscopic
361 observation and evidenced with fluorescence *in situ* hybridisation (FISH; Seitaj et al., 2015).
362 Cores from all stations were examined with FISH in March, May, August and November, and
363 cable bacteria were detected with this technique at ST1 and ST3 in March and May (Seitaj et
364 al., 2015). Conversely, FISH did not give any indication of cable bacteria at ST2. However,
365 there is evidence that the presence of cable bacteria in the basin may be very patchy (Seitaj
366 et al., 2015, 2017). Based on the pore water Mn^{2+} and Fe^{2+} depth profiles, the presence of
367 cable bacteria is likely in January at ST1 and in February and March at ST2 (Fig. S1) in
368 addition to their confirmed presence at ST1 and ST3 in March and May (Sulu-Gambari et al.,
369 2016b). The signature of pH, OPD and hydrogen sulfide profiles confirms the presence of
370 cable bacteria at ST2 in March of another sampling year (Seitaj et al., 2015). It is therefore
371 likely that cable bacteria were active throughout winter and spring in 2012 at all stations,
372 although with an important spatial patchiness. This patchiness of the pore water profiles
373 indicates that despite the supposedly spatially similar settling flux of Mn from the water
374 column in winter, the activity of the cable bacteria determines what part of this flux is
375 transformed to Mn^{2+} . In summary, in a context of ample input of solid-phase Mn through the
376 water column and an oxygenated overlying water column, cable bacteria activity is
377 responsible for the intensification of Mn cycling in the surface sediment in winter and early
378 spring.

379 Cable bacteria were not observed in summer and autumn in Lake Grevelingen, and with the
380 beginning of hypoxia, Mn oxides are removed from the sediment, whereas Fe
381 (oxyhydr)oxides are transformed back to FeS (Sulu-Gambari et al., 2016b). In fact, Sulu-
382 Gambari et al. (2017a) presented data of strongly increased total Mn in the suspended
383 matter in the water column in July 2012, suggesting that during summer hypoxia, due to the
384 release of Mn^{2+} from the pore water into the bottom water, accelerated Mn refluxing took
385 place. Mn refluxing has been described for the Chesapeake Bay as settling of Mn oxides
386 leading to further reductive dissolution in the surface sediment (Adelson et al., 2001), and is
387 with one exception (the depth where oxygen is met in the water column) probably similar in
388 Lake Grevelingen (Sulu-Gambari et al., 2017a).

389 Contrary to the classic model, in Lake Grevelingen, seasonal hypoxia (and variability of Mn
390 input) is not the major control on the seasonal variability of Mn^{2+} concentrations in the pore
391 waters. Nevertheless, although not necessarily during summer hypoxia, deeper in the basin,

392 where oxygen concentrations in summer are lower, pore water Mn^{2+} peaks reached higher
393 values. The metabolic activity of cable bacteria explains the strongly increased Mn^{2+}
394 accumulation in the pore waters in some of the cores sampled in winter and early spring.
395 Concerning the gradient of increasing intensity and vertical extent of the pore water Mn^{2+} and
396 Fe^{2+} peaks from ST3 to ST1, Sulu-Gambari et al. (2016a) and Seitaj et al. (2017) ascribe this
397 to the activity of cable bacteria related to the increasing organic matter mineralisation rates
398 from ST3 to ST1 as well as the interference with more abundant macrofauna, competition
399 with other micro-organisms and/or higher oxygen concentrations at the two shallower
400 stations (Sulu-Gambari et al., 2016b). Here, we will investigate to what extent Mn/Ca ratios of
401 benthic foraminifera such as *Ammonia tepida* enable us to reconstruct this variability of pore
402 water Mn^{2+} in the past by first understanding how living foraminifera are recording the
403 complex present conditions.

404

405 **4.2. General aspects regarding Mn/Ca and biomineralization of benthic** 406 **foraminifera**

407 The average Mn/Ca ratio of *Ammonia tepida* shows a significantly higher value at ST1
408 compared to ST2 and ST3. In Petersen et al. (2018), it is argued that the Mn/Ca intra-test
409 (and implicitly also inter-test) variability may be due to three different factors: 1) intrinsic
410 factors such as ontogenetic trends or vital effects, 2) microhabitat effects (active or passive
411 vertical migration), and 3) temporal variability of the environment. The influence of diagenetic
412 coating on the foraminiferal test with Mn carbonates is not considered here because we
413 analysed only live specimens. Moreover, specimens were cleaned according to a specific
414 protocol followed by LA-ICP-MS data treatment resulting in a Mn/Ca signal of the (biogenic)
415 calcite (Guo et al., 2019). The same three factors have to be evoked here, in addition to
416 spatial variability of the environment, i.e., differences between the three stations. Concerning
417 intrinsic Mn/Ca intra-test variability for *A. tepida*, directly related to the biomineralization
418 process, it was shown that 11-25 % variability occurs in newly calcified chambers under
419 constant laboratory conditions for the range of dissolved Mn concentrations found in our
420 study area (10-100 $\mu\text{mol/L}$; based on data of Barras et al., 2018; further explanation in
421 Petersen et al., 2018). The higher average intra-test variability of 45 % RSD in comparison to
422 this intrinsic variability led Petersen et al. (2018) to the conclusion that it is possible to trace
423 elemental variability based on intra- and inter-specimen Mn/Ca comparisons of *A. tepida*.

424 Since *A. tepida* has an estimated longevity of one to two years (Goldstein and Moodley,
425 1993; Morvan et al., 2006), we estimate that it calcifies during several successive seasons.
426 However, during the foraminiferal lifespan, chamber addition is supposedly not regular, and

427 could be accelerated during short periods of favorable conditions, for example in response to
428 increased food supply (e.g., Jorissen, 1988). Conversely, when conditions are less favorable,
429 e.g., in winter, when primary production is minimal, and less organic matter arrives at the
430 sediment surface, it is possible that construction of new chambers is occurring less often, or
431 may even not take place at all. At ST1, adult living *A. tepida* specimens were only
432 encountered in larger numbers from March to July 2012 (Richirt et al., in prep.). This
433 observation strongly suggests that at ST1, the *A. tepida* population disappears in late
434 summer, due to anoxia (and possibly due to free sulfide at shallow depth in the sediment,
435 Seitaj et al., 2015), and repopulates the site in (late) winter. Therefore, we suggest that these
436 foraminifera started calcifying in (late) winter, and have progressively added chambers over a
437 ~6 month period. In fact, the faunal data collected by Richirt et al. (in prep.) show an ongoing
438 size increase of the population from March to July. It appears therefore that the later calcified
439 parts of the test will be representative for the summer conditions, whereas the earliest parts
440 of the tests may have registered the late winter and/or early spring conditions. Conversely,
441 the year-round presence (with high standing stocks) of *A. tepida* at ST2 and ST3 (Richirt et
442 al., in prep.), and their significantly larger size (Tab. 1) suggest that these specimens have
443 calcified over longer periods of time. This implies that the specimens collected at stations
444 ST2 and ST3 would have registered a (much) larger part of the (inter)annual cycle. In
445 summary, although the last chamber(s) of the foraminifer is (are) supposed to have
446 registered the conditions prevailing in the weeks (to months) prior to sampling, the test as a
447 whole may have integrated environmental conditions over a (much) longer period, of 3 to 6
448 months (ST1) possibly even up to 12 months or more (ST2 and ST3). Because of the
449 trochospiral coiling and the lamellar character of the tests of *A. tepida*, the LA-ICP-MS
450 measurement made at the central part of the test represents an average of a large number of
451 chambers, representative of the total life history of the individual.

452 As a shallow infaunal taxon, *A. tepida* prefers a microhabitat close to the sediment-water
453 interface (SWI), where most of its chamber addition probably takes place (e.g., Thibault de
454 Chanvalon et al., 2015; Cesbron et al., 2016). Active or passive transport processes can lead
455 to the presence of living individuals in deeper layers (see section 4.4). Considering the Mn^{2+}
456 pore water profiles (Fig. S1), it appears that at all three stations, throughout the year, Mn^{2+}
457 concentrations are mostly zero at the SWI and rapidly increase immediately below the
458 sediment surface during certain periods. In fact, maximum Mn^{2+} values are often found
459 between 1 and 3 cm depth during winter, but are situated between 0-0.5 cm in hypoxic
460 summer months. Even if a steep gradient of pore water Mn^{2+} is present in the first cm below
461 the sediment surface, if *A. tepida* calcifies in the well oxygenated niches very close to the
462 sediment surface, it should normally not be confronted with high concentrations of Mn^{2+} , and

463 only chambers calcified slightly deeper should show increased Mn/Ca ratios. However, on
464 the basis of the strongly increased total Mn in water column suspended matter in July, Sulu-
465 Gambari et al. (2017a) concluded that during summer hypoxia Mn^{2+} is released from the
466 surface sediment into the water column (see section 4.1). Evidently, this process of Mn-
467 refluxing must have been strongest at the most hypoxic station ST1, but the data show that
468 also at the other two stations total Mn in water column suspended matter was increased by
469 two orders of magnitude in summer compared to winter months (Fig. 3 and Tab. S2 in Sulu-
470 Gambari et al., 2017a). It appears therefore that at the three stations, abundant Mn^{2+} must
471 have been present in the foraminiferal niches close to the SWI during summer hypoxia
472 (immediately prior to our sampling).

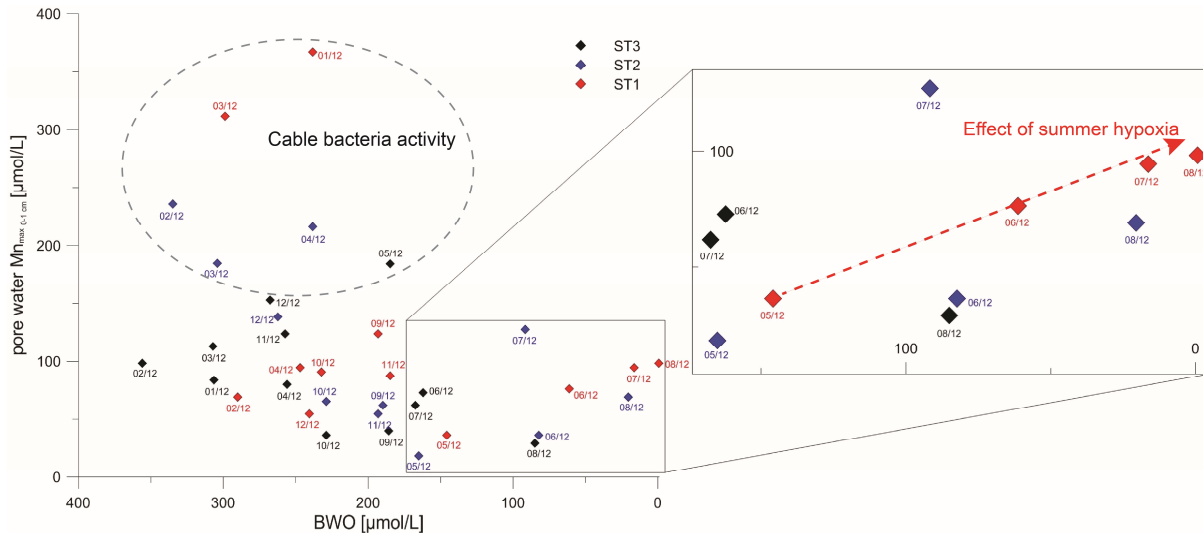
473

474 **4.3. Foraminiferal Mn/Ca response to summer hypoxia and cable bacteria** 475 **activity**

476 Specimens collected in July 2012 showed significant differences in Mn/Ca between the three
477 sampling stations. Compared to ST2 and ST3, much more specimens of station ST1 showed
478 elevated Mn/Ca ratios. Mn/Ca ratios were significantly higher in the central part of the test
479 and also for all measurements on separate individuals taken together (later chambers and
480 central part, Fig. 3 and 4A,D). In fact, the mean Mn/Ca value of 0.36 mmol/mol for ST1 is
481 about two times higher than those of ST2 (0.18 mmol/mol) and ST3 (0.20 mmol/mol). The
482 difference is much larger than could be accounted for by intrinsic (intra-test) variability (11-25
483 %, observed in the study of Barras et al., 2018, under laboratory conditions). This suggests
484 that the difference in Mn/Ca of *A. tepida* between ST1 and the other two stations is reflecting
485 higher Mn^{2+} concentrations in the surface sediment.

486 In Fig. 7, we plotted for each station and for each sampling campaign (i.e., each month), the
487 maximum pore water Mn^{2+} concentration in the topmost centimeter of the sediment against
488 the BWO concentration (data from Hagens et al., 2015; Sulu-Gambari et al., 2016a,b,
489 2017b,c; Seitaj et al., 2017). The plot shows that increased Mn^{2+} concentration is mainly
490 caused by two different processes. First, the data in the upper left part of the plot show a
491 combination of high pore water Mn^{2+} and high BWO concentration. These data correspond to
492 the winter and (early) spring months when cable bacteria activity caused strongly increased
493 Mn^{2+} concentrations. Second, in the right part of the diagram, some data points show a
494 combination of low BWO conc. and relatively increasing Mn^{2+} contents at ST1. In our opinion,
495 these data represent summer hypoxia/anoxia (see previous sections for further explanation
496 which is based on total Mn in water column suspended matter). The diagram also shows that
497 Mn^{2+} concentrations may reach much higher levels in winter (due to cable bacteria activity

498 and increased input of Mn from the water column) than in summer (due to seasonal hypoxia).
 499 Nevertheless, although somewhat masked by the much higher winter/ spring Mn²⁺ values
 500 related to cable bacteria activity, a trend of increasing pore water Mn²⁺ with decreasing BWO
 501 conc. can be observed at ST1 for the summer months (inset in Fig. 7).



502

503 Figure 7. Pore water Mn²⁺ (maximum for depth 0-1 cm) in function of BWO concentration for the three stations. High pore water
 504 Mn²⁺ values associated with cable bacteria activity are indicated by the dashed ellipse. The inset on the right presents values
 505 measured in summer months for which at ST1 an increasing trend is observed. Data from Hagens et al. (2015), Sulu-Gambari
 506 et al. (2016a,b, 2017b,c) and Seitaj et al. (2017). The entire pore water Mn²⁺ profiles are displayed in Figure S1.

507

508 It is interesting to notice that the strongly increased Mn²⁺ concentrations in winter/spring were
 509 mostly situated slightly deeper in the sediment, in the 0.5-1.0 cm level, as opposed to the
 510 summer Mn²⁺ maxima, which were always measured immediately below the sediment
 511 surface, in the 0-0.5 cm sample layer (Fig. S1). The more superficial character of the Mn²⁺
 512 peaks related to summer hypoxia increases the probability that they are recorded in the tests
 513 of foraminifera calcifying close to the SWI, in spite of the fact that the maximum values are
 514 much lower than in winter. Since a substantial part of the specimens (11 out of 26 specimens
 515 for which the last chambers were measured; Tab. 4 and Fig. 5) showed increased Mn/Ca
 516 ratios in the last chambers, it appears that the Mn²⁺ maxima due to summer hypoxia have
 517 indeed been registered. The lack of this signal in the remaining 15 specimens may be due to
 518 the fact that these specimens did not calcify any new chambers after the onset of hypoxia, or
 519 (at stations ST2 and ST3) calcified the last chambers at the SWI (corresponding to bottom
 520 water sediment samples), where Mn²⁺ concentrations were still much lower than at some
 521 mm's depth in the sediment.

522 Regarding the winter/early spring Mn^{2+} maximum, related to cable bacteria activity, we
523 suggest that this has not been registered in one of the last chambers, since several months
524 had passed when the foraminifera were sampled in July 2012. However, increased Mn^{2+}
525 related to cable bacteria activity may have caused increased values in earlier chambers,
526 which should cause an increase of the Mn/Ca ratio in the central part of the test, which
527 represent an average value for the entire growth period(s) of the individual. In fact, at ST1
528 nine out of the 13 specimens had increased values in the central part of test, compared to
529 two out of 13 specimens at ST2 and zero out of nine specimens at ST3 (Tab. 4 and Fig. 5).
530 At ST1, the Mn^{2+} concentration in March, when cable bacteria were actually observed, was
531 more than twice as high as the peaks of ST2 and ST3, and concentrations exceeded 250
532 $\mu\text{mol/L}$ in the 0-1 cm depth interval, which was never reached at the other stations (Fig. 7).
533 The decreasing trend in maximum pore water Mn^{2+} from ST1 to ST2 and ST3 has been
534 attributed to decreasing cable bacteria activity towards shallower waters for reasons that
535 could be indirectly attributed to contrasting BWO concentrations (see section 4.1; Sulu-
536 Gambari et al., 2016a,b; Seitaj et al., 2017). At ST2, there are some indications for the
537 influence of cable bacteria activity on the pore water Mn^{2+} peak for February, March and April
538 2012 (Fig. S1). Except for April 2012, the Mn^{2+} maxima were positioned slightly deeper in the
539 sediment, and the 0-0.5 cm layer showed only a moderate increase of Mn^{2+} , suggesting that
540 high Mn/Ca ratios could only have been registered in some of the chambers. At ST3, finally,
541 we have indications for the presence of cable bacteria in March and May 2012, but Mn^{2+}
542 concentrations never attained the levels observed at ST1 or ST2. Regarding average Mn/Ca
543 ratios, the statistically significantly higher values from specimens of ST1 in comparison to
544 ST2 and ST3 can be explained by the fact that for some specimens the average is mostly
545 reflecting n-c measurements (as later chambers did not yield results, see Tab.1).
546 Summarizing, it appears that in our samples the Mn/Ca ratios in the central part of the
547 foraminiferal test accurately reflect the bathymetrical trend of increasing Mn^{2+} concentrations
548 due to cable bacteria activity.

549 In order to test whether the Mn/Ca values measured in our *A. tepida* specimens are realistic,
550 we applied the partitioning coefficient of $D= 0.086$ determined for calcite Mn/Ca of *Ammonia*
551 *tepada* by Barras et al. (2018) to calculate the maximum possible Mn/Ca ratios of *A. tepida*
552 based on the pore water Mn and Ca profiles, for specimens calcifying in the topmost cm of
553 the sediment (see supplementary material for further explanation and data). It turned out that
554 the maximum values of Mn/Ca observed in the last chambers were close to the maximum
555 theoretical values expected for June/July. Conversely, the maximum values measured in the
556 central part of the test were a half to almost one order of magnitude lower than the
557 theoretical maximum values. This corroborates our conclusion that the sediment Mn^{2+}

558 maximum was largely coinciding with the foraminiferal microhabitat in summer, whereas it
559 was situated deeper in the sediment in winter.

560

561 **4.4 Potential effect of vertical migration of *Ammonia tepida* on the Mn/Ca** 562 **signal**

563 In the previous section we explained that the differences in Mn/Ca ratios between the three
564 stations show a response to two different processes. High Mn/Ca ratios in the central part of
565 the test appear to reflect increased sediment Mn²⁺ levels due to cable bacteria activity in late
566 winter/spring, whereas high Mn/Ca ratios in the last chambers would rather reflect increased
567 Mn²⁺ levels due to summer hypoxia. An important question is to what degree foraminiferal
568 migration through the upper sediment, either active or passive (by macrofaunal burrowing),
569 may contribute to this pattern. In fact, a number of experimental studies have observed
570 (coastal) benthic foraminifera actively migrating in the surface sediment layer, often in
571 response to gradients in oxygen concentration (Alve and Bernhard, 1995; Duijnsteet al.,
572 2003; Ernst et al., 2005; Ernst and Van Der Zwaan, 2004; Geslin et al., 2004; Gross, 2000;
573 Langezaal et al., 2003; Moodley et al., 1998). Additionally, for *A. tepida*, Maire et al. (2016)
574 observed in the laboratory a lower proportion of active individuals under anoxic than under
575 oxic conditions. Thibault de Chanvalon et al. (2015) suggested that hypoxic BWO conditions
576 induced an upward active migration of *A. tepida* in the surface sediment.

577 According to Petersen et al. (2018), vertical migration of the foraminifera within the surface
578 sediment layer may lead to substantial variability in measured Mn/Ca ratios in time-
579 equivalent chambers of different specimens of *A. tepida* in the same sample. In fact, for
580 some individuals, Petersen et al. (2018) observed strongly varying Mn/Ca ratios in
581 successive chambers of the same individual, which they ascribed to the calcification of the
582 chambers with high Mn/Ca in deeper sediment layers, following active or passive migration
583 of the individual. In the present study, where only two or three measurements were made per
584 specimen, such patterns cannot be evidenced. Nevertheless, our data, which show
585 increased Mn/Ca ratios in response to two different phenomena, suggest that the
586 foraminiferal Mn/Ca signal is to some extent modified by migration of the individuals within
587 the topmost sediment.

588 Concerning the winter/spring Mn²⁺ maxima due to cable bacteria activity, since these maxima
589 were present more profoundly in the sediment, it appears that only foraminifera calcifying
590 slightly deeper in the sediment, following active or passive migration, have registered this
591 phenomenon. This would explain the rather low percentage of foraminifera (11 out of 35
592 specimens, Tab. 4 and Fig. 5) showing increased Mn/Ca in the central part of the test.

593 Conversely, in case of the increased Mn/Ca in the later chambers, related to summer
594 hypoxia, since in this case the increased Mn²⁺ levels also affected the topmost sediment
595 layer, it is not necessary to invoke bioturbation to explain the raised Mn/Ca ratios. This is
596 coherent with the fact that macrofauna was absent at ST1 in July 2012 (Sejtaj et al., 2017),
597 excluding the possibility of passive migration. For this study live specimens have been
598 sampled from the topmost cm of the surface sediment, thus excluding interpretations about
599 active or passive migration based on depth distribution.

600

601 **4.5 Paleocological consequences of the observations of Mn/Ca ratios in** 602 **benthic foraminifera from Lake Grevelingen**

603 The present data show that the registration of the pore water Mn dynamics in the coastal
604 foraminifer *A. tepida* is not straightforward, which is to a large degree due to the high
605 complexity of the Mn cycling itself. The two phenomena leading to strong increases of Mn²⁺
606 concentration in the upper sediment layers, cable bacteria activity and summer hypoxia, are
607 registered for our specimens sampled in summer in the central part and in the last chambers
608 of the test, respectively. However, since at least at ST2 and ST3, where *A. tepida* is present
609 year-round, specimens would have continued to add chambers after the summer hypoxia, in
610 fossil specimens the response to summer hypoxia would not systematically be found in the
611 last added chambers. This restricts the use of foraminiferal Mn/Ca ratios in coastal
612 foraminifera measured by LA-ICP-MS to measurements of the central part of the test, which
613 represents an average value for the whole life history of the individual, including periods with
614 high Mn²⁺ due to cable bacteria activity and due to summer hypoxia.

615 Nevertheless, micro-analytical measurements of successive individual chambers may be
616 highly informative. First of all, we have shown that in spite of the much lower Mn²⁺ levels, the
617 summer hypoxia events are maybe even better inscribed in the foraminiferal calcite as the
618 cable bacteria related Mn²⁺ maxima, the latter being positioned slightly deeper in the
619 sediment. Furthermore, the intensity of cable bacteria activity seems to be strongly related
620 (inversely) with the extent of summer hypoxia. Sulu-Gambari et al. (2016a,b) and Seitaj et al.
621 (2017) describe a gradient of decreasing cable bacteria activity from ST1 to ST3 which they
622 explain by the decrease in anaerobic organic matter remineralisation and associated
623 sulphate reduction with decreasing depth in the basin. In fact, in spite of the high complexity
624 of the Lake Grevelingen ecosystem, we found for our three stations a clear inverse
625 relationship between Mn/Ca ratios in the central part of the test and the extent of bottom
626 water hypoxia (which lasted longer and was more intense at ST1 compared to ST2 and ST3,
627 see Fig. 6). This suggests that Mn/Ca ratios in coastal benthic foraminifera, measured by LA-

628 ICP-MS in the central part of the test, may be an important tool to gain insight into the redox
629 processes of complex coastal ecosystems. For future studies it could be envisaged to
630 disentangle different processes by using a multi-proxy geochemical approach and to analyse
631 other elemental ratios reflecting variability of the S cycle which is also influenced by cable
632 bacteria activity.

633

634 **5. Conclusion**

635 We studied Mn/Ca ratios in living specimens of the benthic foraminiferal species *A. tepida* in
636 the complex environmental setting of Lake Grevelingen. It appears that increased Mn/Ca
637 ratios in some of the specimens reflect mainly two factors:

- 638 1) seasonal increases of pore water Mn^{2+} due to cable bacteria activity in late
639 winter/spring, when the bottom water is well oxygenated and Mn-bearing suspended
640 matter is supplied through the water column, lead to higher foraminiferal Mn/Ca in the
641 central part of the test, which represent an average of the specimen's calcification
642 history.
- 643 2) increased Mn-refluxing in surface sediments due to bottom water hypoxia/anoxia in
644 summer leads to increased Mn/Ca ratios in the last formed of our specimens
645 collected in July.

646 Although the maximum pore water Mn^{2+} concentrations generated by cable bacteria activity
647 are higher than those directly related to hypoxia/anoxia and the duration of the cable bacteria
648 activity in winter is longer than the hypoxia period in summer, the Mn^{2+} peaks related to
649 summer hypoxia are positioned closer to the sediment-water interface. Consequently, there
650 is a higher chance that the latter peaks are registered in the foraminiferal shells.

651 It appears that cable bacteria activity in late winter/spring is more intense at sites which are
652 more affected by the summer hypoxia/anoxia, and it seems that these two factors are at least
653 to some extent related. Therefore, in spite of the complex nature of the formation of the
654 Mn/Ca signal, the inter-site differences in seasonal bottom water oxygenation history are well
655 reflected by the foraminiferal Mn/Ca ratios, with higher Mn/Ca average values at ST1 than at
656 ST2 and ST3.

657 Considering the proxy potential of benthic foraminiferal Mn/Ca ratios, in spite of the
658 extremely complex environmental context of Lake Grevelingen (as in comparable coastal
659 ecosystems), the signature measured in the central part of the test could be a potential proxy
660 for the overall redox state of manganese. Although the Mn/Ca ratios of *A. tepida* cannot be

661 explained as a direct response to cable bacteria activity, or to bottom water hypoxia, the
662 close linkage between these two processes makes that foraminiferal Mn/Ca could
663 nevertheless be a powerful indirect proxy for the overall redox state of the basin.
664 Furthermore, the analysis of successive individual chambers may provide more precise
665 insight into seasonal cycles of redox elements. In this respect a multi-proxy approach may be
666 helpful to further disentangle the different processes leading to the Mn/Ca signal as well as
667 calcification periods of individual coastal benthic foraminifera.

668

669

670 **6. Acknowledgements**

671 We are grateful to the crews of the sampling campaigns at Lake Grevelingen as well as the
672 crew of the R/V *Luctor* (Peter Coomans and Marcel Kristalijn). Moreover, Fatimah Sulu-
673 Gambari, Dorina Seitaj and Mathilde Hagens are thanked sincerely for providing the water
674 column and pore water data. This study was financially supported by the Darwin Center for
675 Biogeosciences and the European Research Council under the European Union's Seventh
676 Framework Programme (FP/2007-2013) through ERC Grants 306933 to FJRM and 278364
677 to CPS. We are thankful to the Region Pays de la Loire for financing the MADONA project,
678 including the PhD allocation of JP.

679

- 681 Adelson, J.M., Helz, G.R., Miller, C. V., 2001. Reconstructing the rise of recent coastal
682 anoxia; molybdenum in Chesapeake Bay sediments. *Geochim. Cosmochim. Acta* 65,
683 237–252. [https://doi.org/10.1016/S0016-7037\(00\)00539-1](https://doi.org/10.1016/S0016-7037(00)00539-1)
- 684 Algeo, T.J., Lyons, T.W., 2006. Mo-total organic carbon covariation in modern anoxic marine
685 environments: Implications for analysis of paleoredox and paleohydrographic conditions.
686 *Paleoceanography* 21. <https://doi.org/10.1029/2004PA001112>
- 687 Alve, E., Bernhard, J.M., 1995. Vertical migratory response of benthic foraminifera to
688 controlled oxygen concentrations in an experimental mesocosm. *Mar. Ecol. Prog. Ser.*
689 116, 137–152. <https://doi.org/10.3354/meps116137>
- 690 Bannink, B.A., van der Meulen, J.H.M., Nienhuis, P.H., 1984. Lake Grevelingen: from an
691 estuary to a saline lake. An introduction. *Netherlands J. Sea Res.* 18, 179–190.
- 692 Barker, S., Greaves, M., Elderfield, H., 2003. A study of cleaning procedures used for
693 foraminiferal Mg/Ca paleothermometry. *Geochemistry, Geophys. Geosystems* 4, 8407.
694 <https://doi.org/10.1029/2003GC000559>
- 695 Barmawidjaja, D.M., Vanderzwaan, G.J., Jorissen, F.J., Puskaric, S., 1995. 150 years of
696 eutrophication in the northern Adriatic Sea: evidence from a benthic foraminiferal record.
697 *Mar. Geol.* 122, 367–384. [https://doi.org/10.1016/0025-3227\(94\)00121-Z](https://doi.org/10.1016/0025-3227(94)00121-Z)
- 698 Barras, C., Mouret, A., Nardelli, M.P., Metzger, E., Petersen, J., La, C., Filipsson, H.L.,
699 Jorissen, F.J., 2018. Experimental calibration of manganese incorporation in
700 foraminiferal calcite. *Geochim. Cosmochim. Acta* 237, 49–64.
- 701 Bernhard, J.M., Ostermann, D.R., Williams, D.S., Blanks, J.K., 2006. Comparison of two
702 methods to identify live benthic foraminifera: A test between Rose Bengal and
703 CellTracker Green with implications for stable isotope paleoreconstructions.
704 *Paleoceanography* 21, PA4210. <https://doi.org/10.1029/2006PA001290>
- 705 Breit, G.N., Wanty, R.B., 1991. Vanadium accumulation in carbonaceous rocks: A review of
706 geochemical controls during deposition and diagenesis. *Chem. Geol.* 91, 83–97.
707 [https://doi.org/10.1016/0009-2541\(91\)90083-4](https://doi.org/10.1016/0009-2541(91)90083-4)
- 708 Breitburg, D., Levin, L.A., Oschlies, A., Grégoire, M., Chavez, F.P., Conley, D.J., Garçon, V.,
709 Gilbert, D., Gutiérrez, D., Isensee, K., Jacinto, G.S., Limburg, K.E., Montes, I., Naqvi,
710 S.W.A., Pitcher, G.C., Rabalais, N.N., Roman, M.R., Rose, K.A., Seibel, B.A.,
711 Telszewski, M., Yasuhara, M., Zhang, J., 2018. Declining oxygen in the global ocean
712 and coastal waters. *Science* (80-.). 359, eaam7240.
713 <https://doi.org/10.1126/science.aam7240>
- 714 Cesbron, F., Geslin, E., Jorissen, F.J., Delgard, M.L., Charrieau, L., Deflandre, B., Jézéquel,
715 D., Anschutz, P., Metzger, E., 2016. Vertical distribution and respiration rates of benthic
716 foraminifera: contribution to aerobic remineralization in intertidal mudflats covered by
717 *Zostera noltei* meadows. *Estuar. Coast. Shelf Sci.* 179, 23–38.
718 <https://doi.org/10.1016/j.ecss.2015.12.005>
- 719 Conley, D.J., 2002. Hypoxia in the Baltic Sea and Basin-Scale Changes in Phosphorus
720 Biogeochemistry. *Environ. Sci. Technol.* 36, 5315–5320.
721 <https://doi.org/10.1021/es025763w>
- 722 Conley, D.J., Carstensen, J., Ærtebjerg, G., Christensen, P.B., Dalsgaard, T., Hansen,
723 J.L.S., Josefson, A.B., 2007. Long-Term Changes and Impacts of Hypoxia in Danish
724 Coastal Waters. *Ecol. Appl.* 17, S165–S184.
- 725 Cooper, S.R., Brush, G.S., 1991. Long-Term History of Chesapeake Bay Anoxia. *Science*
726 (80-.). 254, 992–996.
- 727 de Nooijer, L.J., Hathorne, E.C., Reichart, G.J., Langer, G., Bijma, J., 2014. Variability in
728 calcitic Mg/Ca and Sr/Ca ratios in clones of the benthic foraminifer *Ammonia tepida*.
729 *Mar. Micropaleontol.* 107, 32–43. <https://doi.org/10.1016/j.marmicro.2014.02.002>
- 730 Diaz, R.J., Rosenberg, R., 2008. Spreading dead zones and consequences for marine
731 ecosystems. *Science* (80-.). 321, 926–929. <https://doi.org/10.1126/science.1156401>
- 732
- 733

734 Diz, P., Barras, C., Geslin, E., Reichart, G.J., Metzger, E., Jorissen, F., Bijma, J., 2012.
735 Incorporation of Mg and Sr and oxygen and carbon stable isotope fractionation in
736 cultured *Ammonia tepida*. Mar. Micropaleontol. 92–93, 16–28.
737 <https://doi.org/10.1016/j.marmicro.2012.04.006>

738 Duijnste, I.A.P., Ernst, S.R., Van Der Zwaan, G.J., 2003. Effect of anoxia on the vertical
739 migration of benthic foraminifera. Mar. Ecol. Prog. Ser. 246, 85–94.
740 <https://doi.org/10.3354/meps246085>

741 Eggins, S.M., Kinsley, L.P.J., Shelley, J.M.G., 1998. Deposition and element fractionation
742 processes during atmospheric pressure laser sampling for analysis by ICP-MS. Appl.
743 Surf. Sci. 127–129, 278–286. [https://doi.org/10.1016/S0169-4332\(97\)00643-0](https://doi.org/10.1016/S0169-4332(97)00643-0)

744 Ernst, S., Van Der Zwaan, B., 2004. Effects of experimentally induced raised levels of
745 organic flux and oxygen depletion on a continental slope benthic foraminiferal
746 community. Deep. Res. Part I Oceanogr. Res. Pap. 51, 1709–1739.
747 <https://doi.org/10.1016/j.dsr.2004.06.003>

748 Ernst, S., Bours, R., Duijnste, I., Van der Zwaan, B., 2005. Experimental effects of an
749 organic matter pulse and oxygen depletion on a benthic foraminiferal shelf community.
750 J. Foraminifer. Res. 35, 177–197. <https://doi.org/10.2113/35.3.177>

751 Fennel, K., Testa, J.M., 2018. Biogeochemical Controls on Coastal Hypoxia. Ann. Rev. Mar.
752 Sci. <https://doi.org/10.1146/annurev-marine-010318-095138>

753 Geslin, E., Heinz, P., Jorissen, F., Hemleben, C., 2004. Migratory responses of deep-sea
754 benthic foraminifera to variable oxygen conditions: Laboratory investigations. Mar.
755 Micropaleontol. 53, 227–243. <https://doi.org/10.1016/j.marmicro.2004.05.010>

756 Gilbert, D., Rabalais, N.N., Díaz, R.J., Zhang, J., 2010. Evidence for greater oxygen decline
757 rates in the coastal ocean than in the open ocean. Biogeosciences 7, 2283–2296.
758 <https://doi.org/10.5194/bg-7-2283-2010>

759 Glock, N., Eisenhauer, A., Liebetrau, V., Wiedenbeck, M., Hensen, C., Nehrke, G., 2012.
760 EMP and SIMS studies on Mn/Ca and Fe/Ca systematics in benthic foraminifera from
761 the Peruvian OMZ: A contribution to the identification of potential redox proxies and the
762 impact of cleaning protocols. Biogeosciences 9, 341–359. <https://doi.org/10.5194/bg-9-341-2012>

763

764 Goldstein, S.T., Moodley, L., 1993. Gametogenesis and the life cycle of the foraminifer
765 *Ammonia beccarii* (Linné) forma *tepida* (Cushman). J. Foraminifer. Res. 23, 213–220.

766 Groeneveld, J., Filipsson, H.L., 2013. Mg/Ca and Mn/Ca ratios in benthic foraminifera: the
767 potential to reconstruct past variations in temperature and hypoxia in shelf regions.
768 Biogeosciences 10, 5125–5138. <https://doi.org/10.5194/bg-10-5125-2013>

769 Gross, O., 2000. Influence of temperature, oxygen and food availability on the migrational
770 activity of bathyal benthic foraminifera: Evidence by microcosm experiments.
771 Hydrobiologia 426, 123–137. <https://doi.org/10.1023/A:1003930831220>

772 Guo, X., Xu, B., Burnett, W.C., Yu, Z., Yang, S., Huang, X., Wang, F., Nan, H., Yao, P., Sun,
773 F., 2019. A potential proxy for seasonal hypoxia: LA-ICP-MS Mn/Ca ratios in benthic
774 foraminifera from the Yangtze River Estuary. Geochim. Cosmochim. Acta 245, 290–
775 303. <https://doi.org/10.1016/j.gca.2018.11.007>

776 Hagens, M., Slomp, C.P., Meysman, F.J.R., Seitaj, D., Harlay, J., Borges, A. V., Middelburg,
777 J.J., 2015. Biogeochemical processes and buffering capacity concurrently affect
778 acidification in a seasonally hypoxic coastal marine basin. Biogeosciences 12, 1561–
779 1583. <https://doi.org/10.5194/bg-12-1561-2015>

780 Itoh, N., Tani, Y., Nagatani, T., Soma, M., 2003. Phototrophic activity and redox condition in
781 Lake Hamana, Japan, indicated by sedimentary photosynthetic pigments and
782 molybdenum over the last ~250 years. J. Paleolimnol. 29, 403–422.
783 <https://doi.org/10.1023/A:1024407210928>

784 Jorissen, F.J., 1988. Benthic foraminifera from the Adriatic Sea; Principles of phenotypic
785 variation. Utr. Micropaleontologac Bull. 37, 174pp.

786 Jorissen, F.J., Barmawidjaja, D.M., Puskaric, S., Van der Zwaan, G.J., 1992. Vertical
787 distribution of benthic foraminifera in the northern Adriatic Sea : The relation with the
788 organic flux. Mar. Micropaleontol. 19, 131–146.

789 Koho, K.A., de Nooijer, L.J., Reichart, G.J., 2015. Combining benthic foraminiferal ecology
790 and shell Mn/Ca to deconvolve past bottom water oxygenation and paleoproductivity.
791 *Geochim. Cosmochim. Acta* 165, 294–306. <https://doi.org/10.1016/j.gca.2015.06.003>
792 Koho, K.A., de Nooijer, L.J., Fontanier, C., Toyofuku, T., Kazumasa, O., Kitazato, H.,
793 Reichart, G.-J., 2017. Benthic foraminiferal Mn/Ca ratios reflect microhabitat
794 preferences. *Biogeosciences* 14, 3067–3082. <https://doi.org/10.5194/bg-2016-547>
795 Langezaal, A.M., Ernst, S.R., Haese, R.R., Van Bergen, P.F., Van Der Zwaan, G.J., 2003.
796 Disturbance of intertidal sediments: The response of bacteria and foraminifera. *Estuar.
797 Coast. Shelf Sci.* 58, 249–264. [https://doi.org/10.1016/S0272-7714\(03\)00078-7](https://doi.org/10.1016/S0272-7714(03)00078-7)
798 Maire, O., Barras, C., Gestin, T., Nardelli, M.-P., Romero-Ramirez, A., Duchêne, J.-C.,
799 Geslin, E., 2016. How does macrofaunal bioturbation influence the vertical distribution of
800 living benthic foraminifera? *Mar. Ecol. Prog. Ser.* 561, 83–97.
801 Malkin, S.Y., Rao, A.M., Seitaj, D., Vasquez-Cardenas, D., Zetsche, E.-M., Hidalgo-Martinez,
802 S., Boschker, H.T., Meysman, F.J., 2014. Natural occurrence of microbial sulphur
803 oxidation by long-range electron transport in the seafloor. *ISME J.* 8, 1843–1854.
804 <https://doi.org/10.1038/ismej.2014.41>
805 McKay, C.L., Groeneveld, J., Filipsson, H.L., Gallego-Torres, D., Whitehouse, M.J.,
806 Toyofuku, T., Romero, O.E., 2015. A comparison of benthic foraminiferal Mn / Ca and
807 sedimentary Mn / Al as proxies of relative bottom-water oxygenation in the low-latitude
808 NE Atlantic upwelling system. *Biogeosciences* 12, 5415–5428.
809 <https://doi.org/10.5194/bg-12-5415-2015>
810 McManus, J., Berelson, W.M., Klinkhammer, G.P., Hammond, D.E., Holm, C., 2005.
811 Authigenic uranium: Relationship to oxygen penetration depth and organic carbon rain.
812 *Geochim. Cosmochim. Acta* 69, 95–108. <https://doi.org/10.1016/j.gca.2004.06.023>
813 Meier, H.E.M., Andersson, H.C., Eilola, K., Gustafsson, B.G., Kuznetsov, I., Müller-Karulis,
814 B., Neumann, T., Savchuk, O.P., 2011. Hypoxia in future climates: A model ensemble
815 study for the Baltic Sea. *Geophys. Res. Lett.* 38, L24608.
816 <https://doi.org/10.1029/2011GL049929>
817 Meysman, F.J.R., Risgaard-Petersen, N., Malkin, S.Y., Nielsen, L.P., 2015. The geochemical
818 fingerprint of microbial long-distance electron transport in the seafloor. *Geochim.
819 Cosmochim. Acta* 152, 122–142. <https://doi.org/10.1016/j.gca.2014.12.014>
820 Mezger, E.M., Nooijer, L.J., Boer, W., Brummer, G.J.A., Reichart, G.J., 2016. Salinity
821 controls on Na incorporation in Red Sea planktonic foraminifera. *Paleoceanography* 31,
822 1562–1582. <https://doi.org/10.1002/2016PA003052>
823 Middelburg, J.J., de Lange, G.J., van der Weijden, C.H., 1987. Manganese solubility control
824 in marine pore waters. *Geochim. Cosmochim. Acta* 51, 759–763.
825 Middelburg, J.J., Levin, L.A., 2009. Coastal hypoxia and sediment biogeochemistry.
826 *Biogeosciences* 6, 3655–3706. <https://doi.org/10.5194/bgd-6-3655-2009>
827 Moodley, L., Van der Zwaan, G.J., Rutten, G.M.W., Boom, R.C.E., Kempers, L., 1998.
828 Subsurface activity of benthic foraminifera in relation to pore water oxygen content:
829 laboratory experiments. *Mar. Micropaleontol.* 34, 91–106.
830 Morvan, J., Debenay, J.P., Jorissen, F., Redois, F., Bénéteau, E., Delplancke, M., Amato,
831 A.S., 2006. Patchiness and life cycle of intertidal foraminifera: Implication for
832 environmental and paleoenvironmental interpretation. *Mar. Micropaleontol.* 61, 131–
833 154. <https://doi.org/10.1016/j.marmicro.2006.05.009>
834 Munsel, D., Kramar, U., Dissard, D., Nehrke, G., Berner, Z., Bijma, J., Reichart, G.J.,
835 Neumann, T., 2010. Heavy metal incorporation in foraminiferal calcite: Results from
836 multi-element enrichment culture experiments with *Ammonia tepida*. *Biogeosciences* 7,
837 2339–2350. <https://doi.org/10.5194/bg-7-2339-2010>
838 Nielsen, L.P., Risgaard-Petersen, N., Fossing, H., Christensen, P.B., Sayama, M., 2010.
839 Electric currents couple spatially separated biogeochemical processes in marine
840 sediment. *Nature* 463, 1071–1074. <https://doi.org/10.1038/nature08790>
841
842
843

844 Petersen, J., Barras, C., Bézou, A., La, C., De Nooijer, L.J., Meysman, F.J.R., Mouret, A.,
845 Slomp, C.P., Jorissen, F.J., 2018. Mn/Ca intra- and inter-test variability in the benthic
846 foraminifer *Ammonia tepida*. *Biogeosciences* 15, 331–348. [https://doi.org/10.5194/bg-](https://doi.org/10.5194/bg-15-331-2018)
847 15-331-2018

848 Pfeffer, C., Larsen, S., Song, J., Dong, M., Besenbacher, F., Meyer, R.L., Kjeldsen, K.U.,
849 Schreiber, L., Gorby, Y.A., El-Naggar, M.Y., Leung, K.M., Schramm, A., Risgaard-
850 Petersen, N., Nielsen, L.P., 2012. Filamentous bacteria transport electrons over
851 centimetre distances. *Nature* 491, 218–221. <https://doi.org/10.1038/nature11586>

852 R Core Team, 2016. R: A language and environment for statistical computing. R Foundation
853 for Statistical Computing, Vienna, Austria.

854 Rabalais, N.N., Turner, R.E., Wiseman, W.J., 2002. Gulf of Mexico Hypoxia, a.k.a. “The
855 Dead Zone.” *Annu. Rev. Ecol. Syst.* 33, 235–263.
856 <https://doi.org/10.1146/annurev.ecolsys.33.010802.150513>

857 Rabalais, N.N., Levin, L. a., Turner, R.E., Gilbert, D., Zhang, J., 2010. Dynamics and
858 distribution of natural and human-caused coastal hypoxia. *Biogeosciences* 7, 585–619.
859 <https://doi.org/10.5194/bgd-6-9359-2009>

860 Rabalais, N.N., Cai, W.-J., Carstensen, J., Conley, D.J., Fryer, B., Hu, X., Quiñones-Rivera,
861 Z., Rosenberg, R., Slomp, C.P., Turner, R.E., Voss, M., Wissel, B., Zhang, J., 2014.
862 Eutrophication-driven deoxygenation in the coastal ocean. *Oceanography* 27, 172–183.
863 <https://doi.org/10.5670/oceanog.2011.65>

864 Rao, A.M.F., Malkin, S.Y., Hidalgo-Martinez, S., Meysman, F.J.R., 2016. The impact of
865 electrogenic sulfide oxidation on elemental cycling and solute fluxes in coastal
866 sediment. *Geochim. Cosmochim. Acta* 172, 265–286.
867 <https://doi.org/10.1016/j.gca.2015.09.014>

868 Reed, D.C., Slomp, C.P., Gustafsson, B.G., 2011. Sedimentary phosphorus dynamics and
869 the evolution of bottom-water hypoxia: A coupled benthic-pelagic model of a coastal
870 system. *Limnol. Oceanogr.* 56, 1075–1092. <https://doi.org/10.4319/lo.2011.56.3.1075>

871 Reichart, G.J., Jorissen, F., Anschutz, P., Mason, P.R.D., 2003. Single foraminiferal test
872 chemistry records the marine environment. *Geology* 31, 355–358.
873 [https://doi.org/10.1130/0091-7613\(2003\)031<0355:SFTCRT>2.0.CO;2](https://doi.org/10.1130/0091-7613(2003)031<0355:SFTCRT>2.0.CO;2)

874 Richirt, J., Riedel, B., Jorissen, F.J., Langlet, D., Barras, C., Meysman, F.J.R., in prep.
875 Temporal variability of benthic foraminiferal faunas related to seasonal anoxia/hypoxia
876 in Lake Grevelingen, Netherlands.

877 Richirt, J., Schweizer, M., Bouchet, V.M.P., Mouret, A., Quinchar, S., Jorissen, F.J., 2019.
878 Morphological distinction of three *Ammonia* phylotypes occurring along the European
879 coasts. *J. Foraminifer. Res.* 49, 77–94.

880 Risgaard-Petersen, N., Revil, A., Meister, P., Nielsen, L.P., 2012. Sulfur, iron-, and calcium
881 cycling associated with natural electric currents running through marine sediment.
882 *Geochim. Cosmochim. Acta* 92, 1–13. <https://doi.org/10.1016/j.gca.2012.05.036>

883 Schneider, C.A., Rasband, W.S., Eliceiri, K.W., 2012. NIH Image to ImageJ: 25 years of
884 image analysis. *Nat. Methods* 9, 671–675. <https://doi.org/10.1038/nmeth.2089>

885 Scholz, F., Siebert, C., Dale, A.W., Frank, M., 2017. Intense molybdenum accumulation in
886 sediments underneath a nitrogenous water column and implications for the
887 reconstruction of paleo-redox conditions based on molybdenum isotopes. *Geochim.*
888 *Cosmochim. Acta* 213, 400–417. <https://doi.org/10.1016/j.gca.2017.06.048>

889 Seitaj, D., Schauer, R., Sulu-Gambari, F., Hidalgo-Martinez, S., Malkin, S.Y., Burdorf,
890 L.D.W., Slomp, C.P., Meysman, F.J.R., 2015. Cable bacteria generate a firewall against
891 euxinia in seasonally hypoxic basins. *Proc. Natl. Acad. Sci. U. S. A.* 112, 13278–13283.
892 <https://doi.org/10.1073/pnas.1510152112>

893 Seitaj, D., Sulu-Gambari, F., Burdorf, L.D.W., Romero-Ramirez, A., Maire, O., Malkin, S.Y.,
894 Slomp, C.P., Meysman, F.J.R., 2017. Sedimentary oxygen dynamics in a seasonally
895 hypoxic basin. *Limnol. Oceanogr.* 62, 452–473. <https://doi.org/10.1002/lno.10434>

896 Slomp, C.P., Malschaert, J.F.P., Lohse, L., van Raaphorst, W., 1997. Iron and manganese
897 cycling in different sedimentary environments on the North Sea continental margin.
898 *Cont. Shelf Res.* 17, 1083–1117.

899

900 Sulu-Gambari, F., Seitaj, D., Behrends, T., Banerjee, D., Meysman, F.J.R., Slomp, C.P.,
 901 2016a. Impact of cable bacteria on sedimentary iron and manganese dynamics in a
 902 seasonally-hypoxic marine basin. *Geochim. Cosmochim. Acta* 192, 49–69.
 903 <https://doi.org/10.1016/j.gca.2016.07.028>

904 Sulu-Gambari, F., Seitaj, D., Meysman, F.J.R., Schauer, R., 2016b. Cable bacteria control
 905 iron-phosphorus dynamics in sediments of a coastal hypoxic basin. *Environ. Sci.*
 906 *Technol.* 50, 1227–1233. <https://doi.org/10.1021/acs.est.5b04369>

907 Sulu-Gambari, F., Roepert, A., Jilbert, T., Hagens, M., Meysman, F.J.R., Slomp, C.P., 2017a.
 908 Molybdenum dynamics in sediments of a seasonally-hypoxic coastal marine basin.
 909 *Chem. Geol.* 466, 627–640. <https://doi.org/10.1016/j.chemgeo.2017.07.015>

910 Sulu-Gambari, F., Seitaj, D., Behrends, T., Banerjee, D., Meysman, F.J.R., Slomp, C.P.,
 911 2017b. Porewater geochemistry in surface sediment at station DOB_S1. *Suppl. to Sulu-*
 912 *Gambari, F al. Impact cable Bact. Sediment. iron manganese Dyn. a Seas. Mar. basin.*
 913 *Geochim. Cosmochim. Acta*, 192(19), 49-69, <https://doi.org/10.1016/j.gca.2016.07.028>.
 914 <https://doi.org/10.1594/PANGAEA.876622>

915 Sulu-Gambari, F., Seitaj, D., Meysman, F.J.R., Schauer, R., Polerecky, L., Slomp, C.P.,
 916 2017c. Porewater geochemistry at site S3, Lake Grevelingen, The Netherlands. *Suppl.*
 917 *to Sulu-Gambari, F al. Cable Bact. Control iron-phosphorus Dyn. sediments a Coast.*
 918 *hypoxic basin. Environ. Sci. Technol.* 50(3), 1227-1233,
 919 <https://doi.org/10.1021/acs.est.5b04369>. <https://doi.org/10.1594/PANGAEA.876140>

920 Thamdrup, B., Fossing, H., Jørgensen, B.B., 1994. Manganese, iron, and sulfur cycling in a
 921 coastal marine sediment. Aarhus Bay, Denmark. *Geochim. Cosmochim. Acta* 58, 5115–
 922 5129.

923 Thibault de Chanvalon, A., Metzger, E., Mouret, A., Cesbron, F., Knoery, J., Rozuel, E.,
 924 Launeau, P., Nardelli, M.P., Jorissen, F.J., Geslin, E., 2015. Two-dimensional
 925 distribution of living benthic foraminifera in anoxic sediment layers of an estuarine
 926 mudflat (Loire estuary, France). *Biogeosciences* 12, 6219–6234.
 927 <https://doi.org/10.5194/bg-12-6219-2015>

928 Tribovillard, N., Riboulleau, A., Lyons, T., Baudin, F., 2004. Enhanced trapping of
 929 molybdenum by sulfurized marine organic matter of marine origin in Mesozoic
 930 limestones and shales. *Chem. Geol.* 213, 385–401.
 931 <https://doi.org/10.1016/j.chemgeo.2004.08.011>

932 Tribovillard, N., Algeo, T.J., Lyons, T., Riboulleau, A., 2006. Trace metals as paleoredox and
 933 paleoproductivity proxies: An update. *Chem. Geol.* 232, 12–32.
 934 <https://doi.org/10.1016/j.chemgeo.2006.02.012>

935 van Helmond, N.A.G.M., Jilbert, T., Slomp, C.P., 2018. Hypoxia in the Holocene Baltic Sea:
 936 Comparing modern versus past intervals using sedimentary trace metals. *Chem. Geol.*
 937 493, 478–490. <https://doi.org/10.1016/j.chemgeo.2018.06.028>

938 Wickham, H., 2009. *ggplot2: elegant graphics for data analysis*. Springer New York, New
 939 York. <https://doi.org/10.1007/978-0-387-98141-3>

940 Zillén, L., Conley, D.J., Andrén, T., Andrén, E., Björck, S., 2008. Past occurrences of hypoxia
 941 in the Baltic Sea and the role of climate variability, environmental change and human
 942 impact. *Earth-Science Rev.* 91, 77–92. <https://doi.org/10.1016/j.earscirev.2008.10.001>

943